ACS OMEGA

http://pubs.acs.org/journal/acsodf

Article

Naringin in Combination with Isothiocyanates as Liposomal Formulations Potentiates the Anti-inflammatory Activity in Different Acute and Chronic Animal Models of Rheumatoid Arthritis

Sangeeta Mohanty,* Ashish Kumar Sahoo, V. Badireenath Konkimalla,* Abhisek Pal, and Sudam Chandra Si

Cite This: *ACS Omega* 2020, 5, 28319−28332

Read Online

ACCESS | Metrics & More | Article Recommendations

ABSTRACT: Combination of drugs is extensively used to treat chronic inflammatory disease. Naringin (NAR), sulforaphane (SFN), and phenethyl isothiocyanate (PEITC) are nutraceuticals with promising anti-inflammatory properties. However, their clinical effectiveness gets hindered because of low aqueous solubility and poor bioavailability. In the current study, two combinations of liposome (NAR + SFN and NAR + PEITC) were prepared and studied thoroughly in different *in vivo* models of acute and chronic models of inflammation. The encapsulation efficiency of NAR, SFN, and PEITC in the combination liposomal formulations (CLFs) prepared with 1,2-dipalmitoyl-*sn*-glycero-3-phosphocholine/cholesterol/1,2-distearoyl-*sn*-glycero-3-phosphoethanolamine -020CN (15:4:1 M ratio) was determined to be 79.8 ± 4.2, 46.5 ± 3.6, and 78.5 ± 3.2%, respectively. The CLFs were characterized by differential scanning calorimetry, X-ray diffraction, dynamic light scattering, and Fourier transform infrared spectroscopy. The physicochemical results showed that the preparations were monodisperse (PDI 0.062−0.248) in water with an average size from 140.5 to 165.6 nm and a zeta potential of −47.3 to −53.3 mV. Dissolution studies *in vitro* showed a slower release of PEITC (>90%, 6 h) in comparison to that of SFN (3 h). Here, we are the first to report the antiarthritic activity of CLF of NAR + SFN and NAR + PEITC in the Freund's complete adjuvant (FCA)-induced arthritic model. At an intraperitoneal dose (375 + 375 μg/mL) for 3 weeks, the NAR + PEITC liposome significantly improves both % paw edema and arthritic score compared to their free drug combinations in FCA rats. Most importantly, hematological and biochemical results showed improved anemic conditions with significant changes in the SGOT, SGPT, and ALP levels. The ELISA results showed similar trends of increased cytokine (IL-10) and decreased inflammation markers (TNF-α, IL-6, IFN-γ). Histological evaluations showing reduction in cell infiltration, pannus formation, and bone and cartilage destruction further confirm and validate the antiarthritic activity of the CLF. This comprehensive study reveals the effectiveness of combination liposomes of poorly soluble anti-inflammatory molecules (NAR, SFN, PEITC) in the treatment of arthritis.

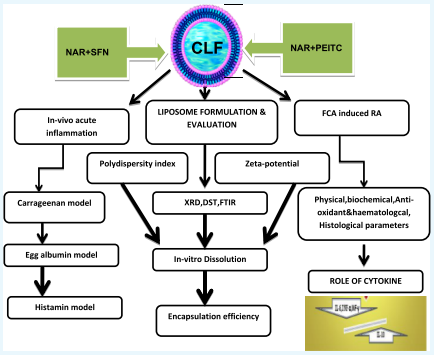

1. INTRODUCTION

Rheumatoid arthritis (RA) is an autoimmune disease that significantly contributes to the global disability burden with higher mortality rates. The incidence rates are continuously on the rise (0.5−1%), affecting 5 million sufferers worldwide.[1] The RA condition is observed in elderly patients with clinical symptoms of progressive destruction of bone and cartilage associated with severe pain and reduced mobility due to chronic inflammation of synovial joints and infiltration by blood derived T cells and macrophages.[2]

Till date, there is no specific drug to treat the RA condition and therefore different categories of drugs such as nonsteroidal anti-inflammatory drugs, disease-modifying antirheumatic drugs (DMARDs), biologics, and Janus kinase inhibitors are often prescribed to obtain relief from the ailing condition. However, prolonged usage of these drugs is often ineffective in chronic conditions and the disease progresses. Therefore, there is a need to develop new modalities and approaches to counteract this condition. A promising strategy for treating RA is the use of a combination of anti-inflammatory/antiarthritic agents. Here, natural products with different mechanisms of action and nonintersecting toxicities emerge as a potential candidate for synergistic combination in various chronic inflammatory diseases.[3] These nutraceuticals can control arthritic inflammation through various pathways that include inhibition of proinflammatory cytokines and chemokines,

Received: September 3, 2020
Accepted: October 12, 2020
Published: October 26, 2020

https://dx.doi.org/10.1021/acsomega.0c04300
ACS Omega 2020, 5, 28319−28332

regulation of the Th17/Treg balance, and induction of anti-inflammatory mediators (IL-4, IL-10).[4]

Naringin (NAR) is a promising citrus flavonoid having versatile pharmacological effects present in the grapefruit.[5] The antioxidant, anti-inflammatory, antimicrobial, anticancer, and antiulcer effects of NAR have been reported in animal models.[6] Previous *in vitro* and *in vivo* studies have showed that it acts through different mechanisms by inhibiting various inflammatory processes such as suppression of interleukin (IL-6), tumor necrosis factor-α (TNF-α), caspase-3, and nuclear factor κ-light-chain-enhancer of activated B cells (NF-κB) in macrophages.[7] In addition, it has gained recognition in the management of chronic inflammatory diseases such as RA. Therefore, NAR brings new hope for the combination therapy of RA. However, the clinical application of NAR is still hindered because of its poor aqueous solubility, low oral bioavailability (8%), short half-life (2.6 h), and cleavage in the gut at harsh pH and enzymatic conditions of the gastrointestinal tract.[8] To alleviate this, existing literature have reported the codelivery approach of NAR with other drugs such as paclitaxel, diltiazem, atorvasin, and DOX.[9] However, NAR is widely used against cancer, diabetes, hypertension, obesity, osteogenesis, osteoporosis, and bone regeneration. A recent review article showed the hepatoprotective and cardioprotective role of NAR, which can be used in the form of functional food or as a phytomedicine in curing various ailments.[10] Isothiocyanates (ITCs) have a general structure of R−N═C═S and are found in cruciferous vegetables such as cabbage, broccoli, cauliflower, brussel sprouts, turnip, and watercress.[10] ITCs are formed by the breakdown of glucosinolates, which are the main constituents of cruciferous vegetables. They are considered to be safe with no adverse effect on humans and possess strong antioxidant, anti-inflammatory, antimicrobial, neuroprotective, and cardioprotective activity.[11] The two major ITCs that have been extensively studied in existing research are phenethyl isothiocyanate (PEITC) and sulforaphane (SFN).

PEITC is a low-molecular-weight (MW = 163.2 g/mol) phytochemical that is fairly lipophilic with a log *P* value of 3.47. The pharmacokinetic feature of PEITC includes first-order linear absorption with a high protein binding nature.[12] A recent study on PEITC (as a potent inhibitor of HDAC1) also demonstrated ameliorated RA by downregulation of TNF-alpha as well as $HDAC_1$ levels in synovial tissue of CFA-induced arthritic rats.[13] On the other hand, SFN is a natural, aliphatic ITC, primarily derived from broccoli, belonging to Brassicaceae family. SFN has also been studied for its inflammatory and antiarthritic activities.[14] A recent report has shown SFN protection against inflammation and joint damage in CFA-induced rats by augmenting TrxR activity, regulating leukocyte activation, and down-regulation of $CD_{11}b$ and $CD_{62}L$ on synovial fluid Ly_6G+ cells.[15] It is also strongly evidenced from literatures that oxidative stress is significantly involved in degradation of cartilage in experimental RA, indicating transcription factor nuclear erythroid-derived 2-like factor (Nrf2) activation to be a vital requirement for limiting cartilage destruction.[16] Nrf2 is also responsible for protecting differentiated chondrocyte in an RA mouse model. Indeed, SFN is a potent activator of Nrf2 and inhibitor of NF-κB and AP-1, which are considered to be the vital transcription factors triggering inflammatory progression in arthritis.[17] In addition, SFN has phlogistic properties that may retard pannus formation. SFN was previously shown to inhibit synovial hyperplasia and T-cell proliferation and to decrease IL-17 and TNF-α production by T cells.[18] The same study also demonstrated that SFN attenuates the severity of experimental RA and the production of auto-antibodies. One of the recent research articles showed that SFN activates the Nrf-2/HO-1 signaling pathway, suppresses diabetes mellitus-induced reactive oxygen species, apoptosis, endoplasmic reticulum stress, and voiding dysfunction.[19] Similarly, another literature review suggests the glaring gap of SFN in breast cancer, for understanding the mechanisms of Nrf-2 homeostasis.[20]

One of the major advantages of SFN in comparison to other ITCs is its higher bioavailability of around 80%, which is due to its molecular weight (MW 177.29), log *P* value of 0.23, its structure, and lipophilicity.[21] Despite SFN showing great promise as an antiarthritic agent, its potential for clinical use is limited because of its short half-life (less than 2 h), unstable nature, and poor encapsulation efficiency (EE).[22] Hence, administration of SFN to attain therapeutic active doses might be problematic. Our previous works on SFN have demonstrated the anti-inflammatory activity using an acute and subchronic model of inflammation and antiarthritic effect in Freund's complete adjuvant (FCA)-induced rats at an oral dose of 5 mg/kg (po) by suppressing proinflammatory cytokines and tissue regeneration.[23,24]

In this scenario, the major challenge of nutraceuticals lies in their pharmacokinetic profile. Consequently, codelivery of multiple antiarthritic natural products *via* a nanocarrier seems a promising approach to further improve the effectiveness of combinatorial drug therapy by inducing synergistic drug actions. Preclinical studies also witnessed that multidrug-loaded nanocarriers can reverse drug resistance more efficiently than conventional combination therapies. Although many platforms are available for nanocarriers, liposomes, approved by the FDA, because of their biocompatible and biodegradable nature, have emerged as an attractive approach for addressing the issues related to poor water solubility and bioavailability.[25] This can encapsulate both hydrophobic and hydrophilic drugs and can release the entrapped drug at designated targets. Particularly, the stealth liposome (PEGylated liposome) is considered to be an efficient drug carrier, which can evade rapid clearance by the reticuloendothelial system of the body. More interestingly, current reports have specified liposomes to be the only platform for nanocarrier-based combinatorial drug delivery, which have been used in clinical trials. Additionally, due to passive targeting and PEGylation, there is reduced uptake of liposomes by the liver and spleen, resulting in increased circulation time.[26] Dual drug-loaded liposomes may accumulate more at the inflamed site, which is secondary to the enhanced permeability and retention (EPR) effect.[27] Most of the combination therapies that have been reported previously in order to combat RA were either using MTX or DMARDS, which requires a high dose, resulting in side effects. However, till date, there are no reports available that report combination therapies using two naturally occurring potent anti-inflammatory phytochemicals (flavonoids with ITC) for targeting the RA condition. Therefore, the aim of the present study is to prepare and characterize combinatorial drug-loaded liposomes for RA treatment.

2. RESULTS AND DISCUSSION

2.1. Formulation Development. The mean particle size, polydispersity index, and zeta potential are crucial parameters to be considered for improved biodistribution and prolonged

https://dx.doi.org/10.1021/acsomega.0c04300
ACS Omega 2020, 5, 28319−28332

pharmacokinetics of encapsulated hydrophobic drugs. Results for the physicochemical characterization of the prepared combination liposomal formulations (CLFs) are summarized in Table 1.

Table 1. Characteristics of CLFs: Particle Size, Polydispersity Index, and Zeta Potential

formulation	particle size (nm)	polydispersity index	zeta potential (mV)
15:0:1 NAR + SFN	147.1 ± 2.8	0.175 ± 0.013	−50.7 ± 0.6
15:4:1 NAR + SFN	155.9 ± 2.9	0.248 ± 0.008	−49.0 ± 0.7
15:9:1 NAR + SFN	161.4 ± 0.8	0.154 ± 0.016	−47.3 ± 1.3
15:0:1 NAR + PEITC	140.5 ± 0.8	0.090 ± 0.011	−53.3 ± 1.1
15:4:1 NAR + PEITC	148.7 ± 1.7	0.062 ± 0.049	−49.8 ± 0.7
15:9:1 NAR + PEITC	165.6 ± 3.5	0.204 ± 0.008	−47.6 ± 0.6

The CLFs had a low particle size in the range from 140.5 to 165.6 nm, with a narrow size distribution ranging from 0.062 to 0.248 and zeta potential values ranging from −47.3 to −53.3 mV, indicating high stability of the formulation with better homogenization of liposomes during extrusion with no aggregation (Figure 1).

Low particle size results in longer circulation time; as a result, higher accumulation of liposomes in inflamed joints may occur, which can improve *in vivo* targeting efficiency.[28] In the present work, we used lipid compositions (1,2-dipalmitoyl-*sn*-glycero-3-phosphocholine (DPPC)/cholesterol/1,2-distearoyl-*sn*-glycero-3-phosphoethanolamine [(DSPE)-020CN] in a 15:0:1/15:4:1/15:9:1 M ratio to prepare NAR + SFN and NAR + PEITC CLFs. However, cholesterol was incorporated to regulate the rigidity/fluidity of the membranes but it decreases the incorporation efficiencies of many drugs. In this context, addition of very low amounts of PEGylated lipids makes them more stable and long-circulating, which enables the drug to stay for many hours in the blood stream.[29] In addition, DSPE-020CN, which differs from DSPE-PEG2000 with the presence of an attached methoxy group ($-OCH_3$) versus an amine group ($-NH_2$) to the PEG chain, the rest being the same (DSPE-020CN *vs* DSPE-PEG2000), is incorporated to modify the liposomal surface in order to have a formulation illustrating a lengthy circulation time so as to potentiate the EPR effect. Although the exact mechanism for retention of liposome is yet unknown, reports suggest that activated synoviocytes are having stronger phagocyte capacity, which may contribute to liposome retention in RA. This phenomenon is known as the "ELVIS" (extra through leaky vasculature and subsequent inflammatory cell-mediated sequestration) effect, which is very similar to the EPR effect in tumors.[30]

2.2. Drug Encapsulation Studies. SFN and PEITC encapsulation is quantified using cycloreactions between ITC and 1,2-benezenedithiol (BDT) as per Zhang *et al.* Briefly, 8 mM of BDT is formed in methanol. Potassium phosphate buffer of pH 8.5 is formed and 1% Triton X-100 is added to it to break down the lipid. The sample (100 μL), 500 μL of buffer, and 500 μL of 8 mM BDT are mixed and heated in a dry bath for 1 h. Then, the solution is allowed to cool at room temperature, centrifuged at 21,000*g* for 10 min, and absorbance of the supernatant is taken at 365 nm. For NAR quantification, 100 μL of liposomes is mixed with 450 μL of methanol and 450 μL of water for 10× dilution so as to solubilize the lipid particles. Absorbance was checked at 283 nm and multiplied 10× to find the concentration of NAR present. Quantification of free drugs NAR, SFN, and PEITC is done at a 15:4:1 lipid ratio.

EE is calculated by the following formula

$$\mathrm{EE} = \frac{\text{actual amount of drug encapsulated}}{\text{total amount of drug added for encapsulation}} \times 100$$

SFN (400 μg/mL), 500 μg/mL of PEITC, and 500 μg/mL of NAR were taken for formulation as these concentrations of drugs did not show any adverse effect on rats, as detected by toxicity studies. To understand the effect of cholesterol in the liposome formulation, three different concentrations of cholesterol were taken and EE was ascertained. It was found that 15:4:1 M ratio of DPPC/Chol/DSPE-020CN showed the best encapsulation for the drugs with an EE of 45.3 ± 1.6 and

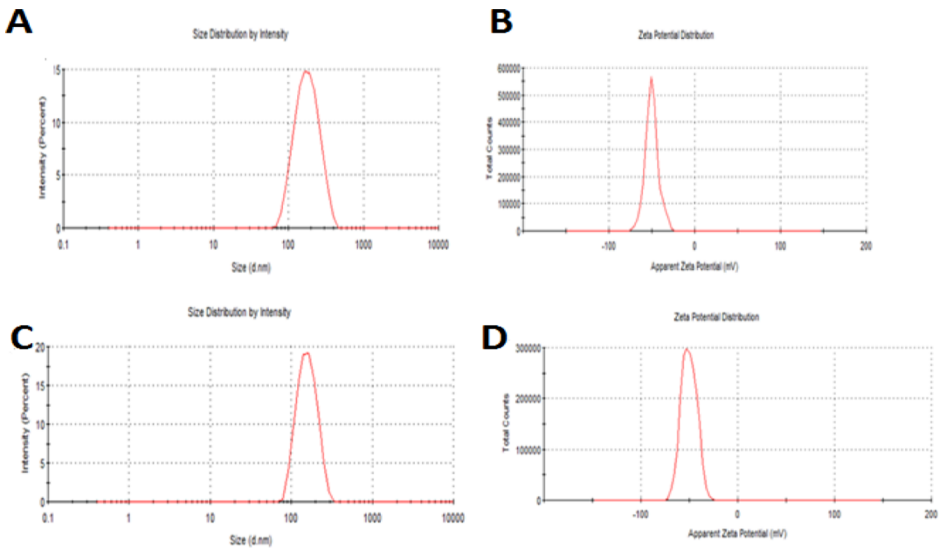

Figure 1. Size distribution (A) and zeta potential curve (B) of NAR + SFN CLF; size distribution (C) and zeta potential curve (D) of NAR + PEITC CLF.

https://dx.doi.org/10.1021/acsomega.0c04300
ACS Omega 2020, 5, 28319−28332

78.±2.7% for SFN and NAR, respectively, in the NAR + SFN combination and 77.7 ± 4.0 and 79.1 ± 3.1% for PEITC and NAR, respectively, in the NAR + PEITC formulation (Tables 2−5). Therefore, this ratio of CLFs (15:4:1 NAR + SFN and 15:4:1 NAR + PEITC) was taken forward for further *in vivo* studies.

Table 2. SFN (400 μg/mL) (2.26 mM) Encapsulation in the NAR + SFN Liposome

lipid ratio (DPPC/Chol/DSPE-020 CN)	concentration of SFN postdialysis (μg/mL)	encapsulation efficiency (%)
15:0:1	158.1 ± 7.7	39.5 ± 1.9
15:4:1	181.1 ± 6.2	45.3 ± 1.6
15:9:1	183.0 ± 9.4	45.6 ± 2.4

Table 3. NAR (500 μg/mL) (689.013 μM) Encapsulation in the NAR + SFN Liposome

lipid ratio (DPPC/Chol/DSPE-020CN)	concentration of NAR postdialysis (μg/mL)	encapsulation efficiency (%)
15:0:1	366.2 ± 14.5	73.2 ± 2.9
15:4:1	394.6 ± 13.3	78.9 ± 2.7
15:9:1	386.2 ± 14.9	77.2 ± 3.0

Table 4. PEITC (500 μg/mL) (3.06 mM) Encapsulation in the NAR + PEITC Liposome

lipid ratio (DPPC/Chol/DSPE-020 CN)	concentration of PEITC postdialysis (μg/mL)	encapsulation efficiency (%)
15:0:1	343.1 ± 19.2	68.6 ± 3.8
15:4:1	388.3 ± 19.9	77.7 ± 4.0
15:9:1	384.2 ± 17.9	76.8 ± 3.6

Table 5. NAR (500 μg/mL) (689.013 μM) Encapsulation in the NAR + PEITC Liposome

lipid ratio (DPPC/Chol/DSPE-020 CN)	concentration of NAR postdialysis (μg/mL)	encapsulation efficiency (%)
15:0:1	370.9 ± 23.3	74.2 ± 4.7
15:4:1	395.4 ± 15.4	79.1 ± 3.1
15:9:1	380.3 ± 17.4	76.1 ± 3.5

2.3. Fourier-Transform Infrared. FTIR is an important analytical tool to predict the interactions between drugs and excipients and the nature of drugs after encapsulation (molecular/crystalline/amorphous).

FTIR spectra corresponding to the free drugs (SFN, NAR), blank liposome, and CLF (15:4:1 NAR + SFN) are represented in Figure 2A. NAR has polyhydroxy groups; hence, on exposure to IR, it exhibits a strong absorption peak in the range of 3000−3500 cm^{-1}. Accordingly, the FTIR spectrum of NAR exhibited characteristic bands at 3421.84 cm^{-1}. Other characteristic bands of NAR included −CH aliphatic at 2930.73 cm^{-1}, phenolic −OH at 1205 and 1363 cm^{-1}, aromatic −OH at 1519 cm^{-1}, and C═O at 1453.16 cm^{-1}.[31] The infrared spectrum of the pure drug SFN showed a characteristic ITC (N═C═S) functional group band at around 2099 cm^{-1}, which is in accordance with the literature by Lieber *et al.*[32] They suggested that ITC peaks can be found at 2140 cm^{-1} or between 2060 and 2105 cm^{-1}. Other peaks of SFN are seen at 3452.33 (−OH), 1231.73 cm^{-1} (C−C), 1368.78 cm^{-1} (C−N), 1422.88 cm^{-1} (−S═O), and 1703 cm^{-1} (C═N), respectively. The blank liposome spectra show characteristic IR peaks of phospholipids at 3410.43 cm^{-1} (−OH), 2919.05 and 2849.49 cm^{-1} ($-CH_2$), 1740.54 cm^{-1} (C═O), and 1093.70 cm^{-1} (PO_2^{-1}) for symmetric vibration stretching.[33] When drugs were incorporated into the liposome, characteristic peaks of both SFN (N═C═S) (in the range of 2060−2105 cm^{-1}) and NAR (in the range of 3000−3500 cm^{-1}) were not seen evidently in CLF. However, there is the presence of a phospholipid peak in reduced intensity with some shift in the peaks as depicted in the IR spectrum of 15:4:1 NAR + SFN CLF. SFN peaks were shifted from 1231.73 to 1244.76 and from 1703 to 1738.12 cm^{-1}. Similar shift in peaks was observed for NAR from 1453.16 to 1468.36 cm^{-1}. The disappearance of drug bands in the CLF demonstrate complete drug encapsulation.

Figure 2B depicts FTIR spectra corresponding to the drugs (NAR, PEITC), blank liposome, and CLF of 15:4:1 NAR + PEITC. A report by Lieber *et al.* suggested that characteristic peaks of ITC (−N═C═S) can be observed either at 2140 cm^{-1} or between 2060 and 2105 cm^{-1}.[34] Accordingly, the main peaks of PEITC appeared at 2115.89 cm^{-1} (−N═C═S), 1348.56 cm^{-1} (C−C), and 1710 cm^{-1} (C═O), respectively.[35] Interestingly, the spectra of CLF (15:4:1 NAR + PEITC) did not show the drug bands. Also, bands appeared in reduced intensity, but no other change was identified. The disappear-

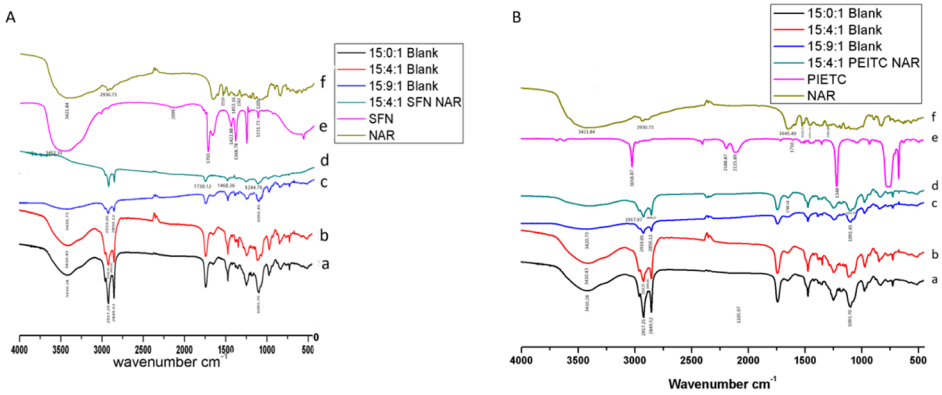

Figure 2. (A) FTIR of CLF of NAR + SFN: (a) 15:0:1 blank liposome, (b) 15:4:1 blank liposome, (c) 15:9:1 blank liposome, (d) 15:4:1 NAR + SFN liposome, (e) pure drug SFN, and (f) pure drug NAR. (B) FTIR of CLF of NAR + PEITC: (a) 15:0:1 blank liposome, (b) 15:4:1 blank liposome, (c) 15:9:1 blank liposome, (d) 15:4:1 NAR + PEITC liposome, (e) pure drug PEITC, and (f) pure drug NAR.

https://dx.doi.org/10.1021/acsomega.0c04300
ACS Omega 2020, 5, 28319−28332

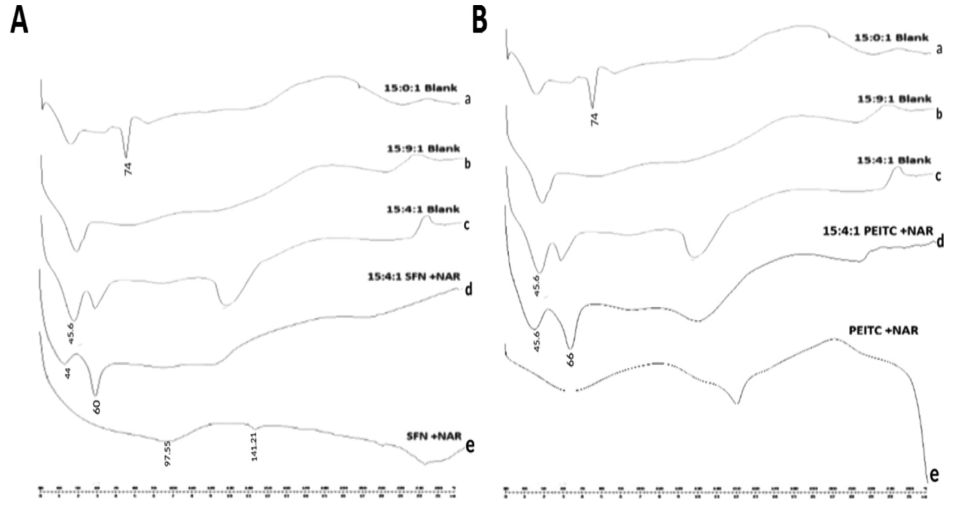

Figure 3. (A) DSC of CLF of NAR + SFN: (a) 15:0:1 blank liposome, (b) 15:9:1 blank liposome, (c) 15:4:1 blank liposome, (d) 15:4:1 NAR + SFN liposome, and (e) combination of pure drugs SFN + NAR. (B) DSC of CLF of NAR + PEITC: (a) 15:0:1 blank liposome, (b) 15:9:1 blank liposome, (c) 15:4:1 blank liposome, (d) 15:4:1 NAR + PEITC liposome, and (e) combination of pure drugs PEITC + NAR.

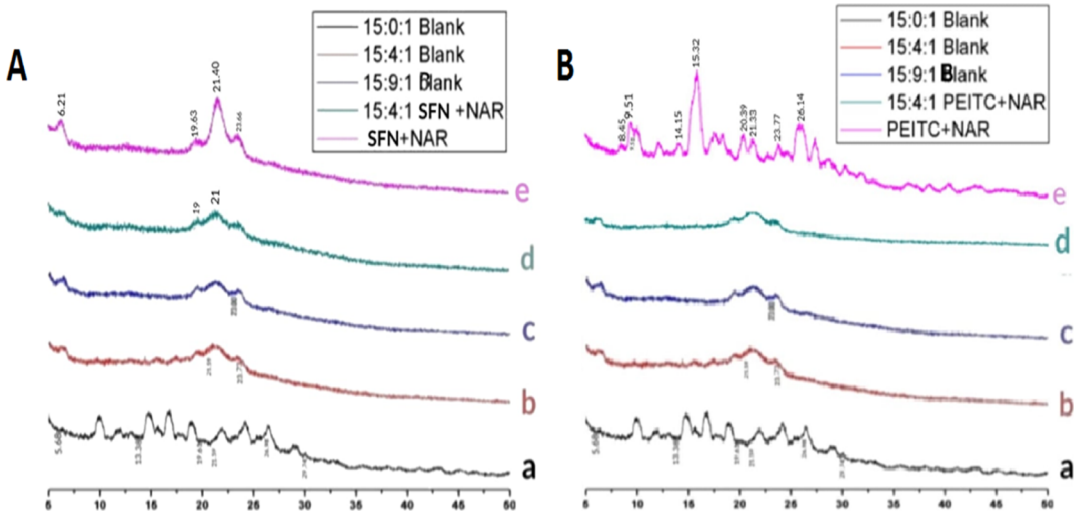

Figure 4. (A) XRD diffraction patterns of CLF of NAR + SFN: (a) 15:0:1 blank liposome, (b) 15:4:1 blank liposome, (c) 15:9:1 blank liposome, (d) 15:4:1 NAR + SFN liposome, and (e) combination of pure drugs NAR + SFN. (B) XRD diffraction patterns of CLF of NAR + PEITC: (a) 15:0:1 blank liposome, (b) 15:4:1 blank liposome, (c) 15:9:1 blank liposome, (d) 15:4:1 NAR + PEITC liposome, and (e) combination of pure drugs NAR + PEITC.

ance of drug bands in the CLF with phospholipids may indicate drug encapsulation.

2.4. Differential Scanning calorimetry. From Figure 3A, it is observed that the differential scanning calorimetry (DSC) thermogram of the blank liposome composed of DPPC/cholesterol/DSPE-020CN in a 15:4:1 M ratio shows a peak at 45.6 °C corresponding to DPPC and for a 15:0:1 M ratio, the peak was seen at 74 °C, which corresponds to the lamellar gel-to-fluid phase transition for DSPE-020CN and in accordance with literature.[36] Previous reports suggested that NAR exhibits two endothermic peaks at 95.51 and at 162.93 °C.[37] Accordingly, the DSC profile for the combination of pure drugs (NAR + SFN) showed endothermic peaks at 97.55 and at 141.21 °C (slight shift). When drugs were encapsulated into the phospholipids, as depicted in the DSC profile of CLF (15:4:1 NAR + SFN), the presence of phospholipid peaks was clearly seen but with a slight shift (from 45.6 to 44 °C). However, drug peaks were not evident and the presence of an extra peak at 60 °C was marked also. The disappearance of drug peaks in the formulated CLF confirms complete drug incorporation into the liposome, which may be due to amorphization. Figure 3B shows the DSC profile showing the combination of pure drugs (NAR + PEITC) observed at 62.93 °C (broadened from 30 to 97 °C) and at 150.88 °C (broadened from 143 to 150.88 °C). However, the DSC profile of our formulated CLF did not show any defined melting point of pure drugs. This may be occurring because of amorphization, but it showed the presence of a phospholipid peak in the DSC thermograms of CLF.

2.5. X-ray Diffractometry. The X-ray diffractometry (XRD) patterns of a pure drug combination, blank liposomes, and the CLF of NAR + SFN are shown in Figure 4A. It represents a number of intense peaks especially for the pure drug combination (NAR + SFN) at 2θ, 6.21, 19.63, 21.40, 21.65, and 23.66°, indicating the crystalline nature of the drugs.[38] XRD thermograms of the phospholipid (DPPC/

https://dx.doi.org/10.1021/acsomega.0c04300
ACS Omega 2020, 5, 28319−28332

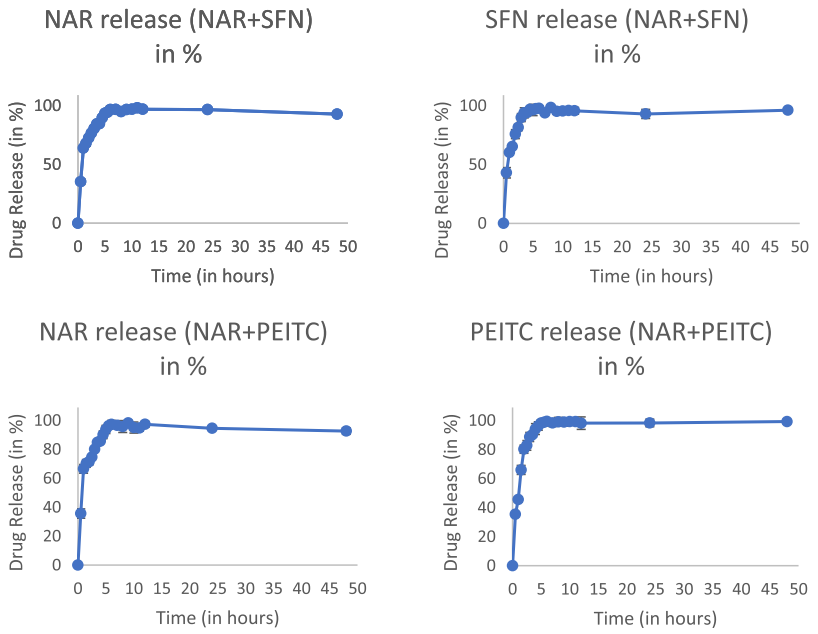

Figure 5. *In vitro* release profile of CLFs.

Table 6. *In Vitro* Release Modeling for the CLF Combination

drugs in coloaded liposome	zero-order $C = K_o t\ R^2$	first-order $\ln C = \ln C_o + K_t\ R^2$	Higuchi order $Q = K_H t^{1/2}\ R^2$	Hixon–Crowell $Q_0^{1/3} - Q_t^{1/3} = K_H C_t\ R^2$	Korsmeyer–Peppas $M_t/M_\infty = K_p t^n\ R^2$	N
NAR in 15:4:1 NAR + SFN	0.734	0.967	0.7887	0.926	0.925	0.748
SFN in 15:4:1 NAR + SFN	0.730	0.976	0.93	0.931	0.922	0.754
NAR in 15:4:1 NAR + PEITC	0.731	0.955	0.921	0.937	0.922	0.74
PEITC in 15:4:1 NAR + PEITC	0.768	0.983	0.941	0.974	0.946	0.768

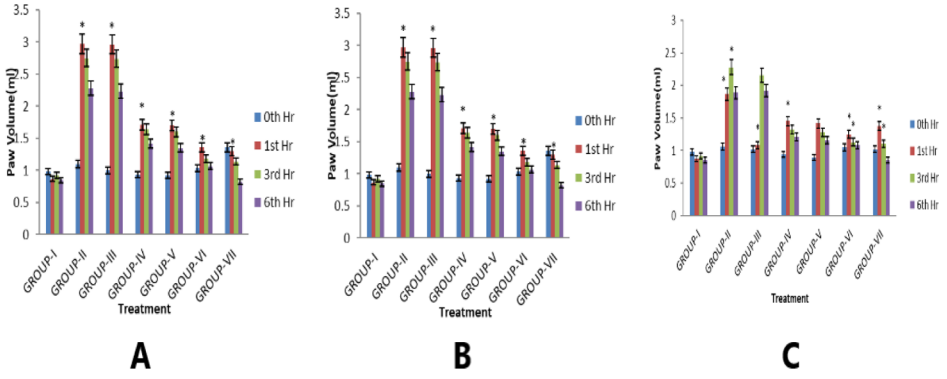

Figure 6. Effect of CLFs on (A) carrageenan-induced hind paw edema, (B) histamine-induced hind paw edema, and (C) egg–albumin-induced hind paw edema in rats.

Chol/DSPE-020CN) were observed at 2θ, 5.68, 13.38, 19.61, 21.59, 26.98, and 29.74°. However, in the CLF of 15:4:1 NAR + SFN, peaks of both phospholipids and pure drugs were seen in the same pattern but with decreased intensity. This difference might be due to the formation of new amorphous phases, which is attributed to complete drug encapsulation.[39]

The XRD pattern of the pure drug combination shows a number of intense peaks especially for NAR and PEITC at 2θ, 8.45, 9.51, 14.15, 15.32, 20.39, 21.33, 23.77, and 26.14°, indicating the crystalline nature of the drugs (Figure 4B).[40]he characteristic peaks of the phospholipid (DPPC/Chol/DSPE-020CN) were observed at 2θ, 5.68, 13.38, 19.61, 21.59, 26.98, and 29.74°. Peaks which were initially seen in the pure drug combination disappeared in the diffractograms of CLF (15:4:1 NAR + PEITC). This confirms the amorphization of both lipids and pure drugs (NAR, PEITC) in the liposomal formulation. It may be due to complete drug encapsulation. However, amorphization increases the solubility and bioavailability of the drugs makes it more efficient for drug targeting.

2.6. *In Vitro* Release Studies. *In vitro* drug release studies are a crucial tread during drug development. The reason is that it not only serves the quality aspects of formulations but also

https://dx.doi.org/10.1021/acsomega.0c04300
ACS Omega 2020, 5, 28319–28332

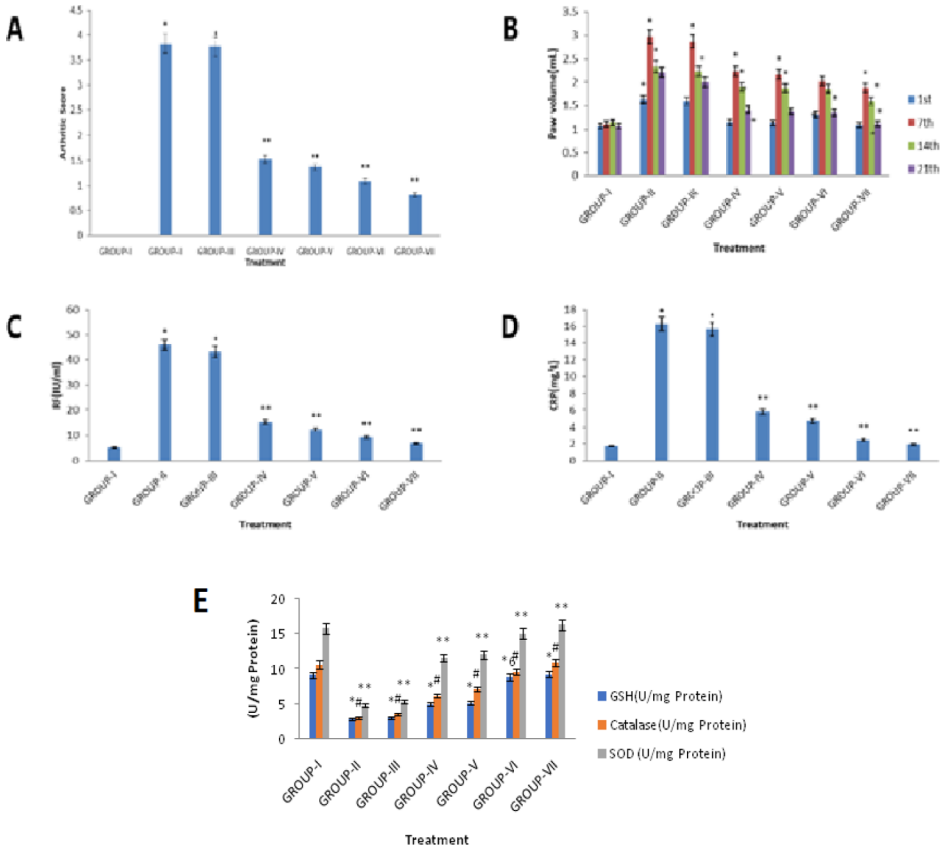

Figure 7. Effect of CLFs on (A) arthritic index of rats, (B) paw volume in FCA-induced arthritic rats, (C) biochemical parameter "RF" in FCA-induced arthritis in rats, (D) biochemical parameter "CRP" in FCA-induced arthritis in rats, and (E) antioxidant enzymes on FCA-induced arthritic rats.

reflects the *in vivo* performance as well. The release studies were carried out in pH 7.4 buffer at room temperature using dialysis bags. Figure 5 summarizes the drug release profiles for both the prepared liposomes up to 6 h. The release data were separately fitted to various kinetic equations, that is, zero order, first order, Higuchi, Hixson−Crowell, and Korsmeyer Peppas model, to predict the kinetics and drug release mechanism (Table 6).

The best fit with the highest regression coefficient (R^2) was found for the well-known equation of the first-order model. SFN gets released in 3 h, which means it stays in the body for fewer hours, the onset of action may be fast, and the response is fast but its kinetics ($t^{1/2}$) will be low. Hence, it shows lesser biological activity as compared to PEITC, which stays in the systemic circulation for longer hours (6 h), demonstrating better controlled activity. However, NAR gets released in 6 h (Figure 5).

2.7. *In Vivo* Efficacy Evaluation in Acute Inflammatory Models in Rat. Mean increase of the carrageenan-treated paw volumes of the foot was noticed at the 0th, 1st, 3rd, and 6th hours (Figure 6A).

The injection of carrageenan into the hind paw of rats causes inflammation signs such as edema, erythema, and hyperalgesia, which occurs in three distinct phases, that is, release of mediators serotonin and histamine in the first phase (0−2 h), kinins in the second phase (3 h), and prostaglandin in the third phase (>4 h).[41] This antiedematous response is reflected in our prepared CLFs (NAR + SFN and NAR + PEITC), which significantly inhibits the paw edema induced by carrageenan in all the three phases as compared to free drugs (combination). This might be due to the factor suggesting the mediator's inhibition activity and COX (cyclo-oxygenase) inhibitory property of NAR, which may be responsible for showing a better anti-inflammatory response.

Another influential mediator is histamine, a potent vasodilator, responsible for expanded vascular permeability.[42] Our results for this acute inflammation study as shown in Figure 6B reveal that both the CLFs significantly suppressed the edematous paw volume produced by histamine, which is attributed to the factor that ITC (SFN and PEITC) possesses a marked anti-inflammatory activity in connection with the antihistaminic property.

The subcutaneous injection of egg albumin in the rat paw results in the development of edema. It may be due to plasma and neutrophil extravasations, increased tissue water, and plasma protein exudations.[43] Both NAR + SFN and NAR + PEITC CLFs showed good anti-inflammatory response by blocking the two mediators for release of histamine and 5HT, which were mainly released by egg-albumin (Figure 6C). However, NAR, a cycloxygenase inhibitor (COX), when combined with SFN and PEITC in liposomal formulation significantly decreases the edema produced by egg albumin.

2.8. *In Vivo* Efficacy Evaluation in Chronic Inflammatory Models in Rat. The arthritic score depicts the combination index of inflammation, nodule formation, and extent of disease spread to other organs. It provides the full picture of disease manifestation. In the affected joints, a normal synovium develops many villous folds with increase in number and size of cells because of colonization of lymphocytes. In addition, inflammation was marked on the nose, ears, tail, hind

https://dx.doi.org/10.1021/acsomega.0c04300
ACS Omega 2020, 5, 28319−28332

Table 7. Effect of CLFs on Serum SGOT, SGPT, and ALP Levels and Hematological Parameters on FCA-Induced Arthritis

formulations	SGOT (U/mL)	SGPT (U/mL)	ALP (U/mL)	Hb (gm/dL)	total WBC Count (thousands/μL)	RBC (million/μL)
group I	75.0	20.52	64.02	16.01	8.03	9.52
group II	165.11	72.03	239.12	8.16	33.21	4.24
group III	163.23	70.2	235.23	9.22	31.0	5.48
group IV	141.01	58.12	182.12	10.23	18.3	6.03
group V	80.23	34.03	63.23	13.8	8.01	7.21
group VI	139.0	52	173.04	11.2	18.02	6.08
group VII	77.21	30.12	67.33	14.06	8.28	9.12

paws, and fore paws. The rats in the adjuvant-induced group having a significantly higher arthritic score of 3.76 ± 0.34 (on days 1, 7, 14, 21) (Figure 7A) than the control rats ($p < 0.05$) demonstrate that FCA immunization successfully induced arthritis in all the experimental rats. On the 10th day, the joints showed a slight swelling and erythema, but it gets fully developed by the 14th day, when severe swelling with redness was noted. Previous data from research claimed that two important parameters for identifying the therapeutic potential of any drug against RA are paw swelling and arthritic index. Hence, use of the right drug combination is one that reduces these clear signs of inflammation. Upon 21 days of treatment, with the combination of free drugs and their coloaded liposome/blank liposome administration, rats in the treated groups showed a maximum reduction in edema and resemblance to a normal paw volume (Figure 7A,B).

The liposomal-treated group produced statistically significant minimization in the arthritic score compared to the disease control group. However, the free drug combination (NAR + SFN/NAR + PEITC) was associated with slowing disease progression, but a marked effect was observed with liposomal administration to a greater extent. No effect was noticed in rats treated with the blank liposome.

Two more important biomarkers of systemic inflammation with antibody production against adjuvant-induced arthritis are C-reactive protein (CRP) and serum rheumatoid factor (RF).[44] CRP is released from liver in inflammatory conditions in response to the action of interleukin (IL-6) and develops antigen presentation. On the other hand, RF generation in arthritis is due to activation of T-cells and B-cells *via* toll-like receptors. In the present experiment, high levels of serum RF (45.77 IU/mL) and serum CRP (16.25 IU/mL) were observed in group II (FCA-treated rats). Also, efficacy differences between CLFs and the free drug combination were marked clearly. Liposomal treatment significantly reduced the increased levels of RF factor and CRP to a normal range (Figure 7C,D) of RF (0−20 IU/mL) and CRP (0−6 mg/dL).[45] The relative reduction of RF factor from 45.77 ± 1.92 to 6.88 ± 0.82 and 12.44 ± 1.02 IU/mL is well marked for the coloaded liposome of NAR + PEITC (dose 375 + 375 μg/mL) and NAR + SFN (dose 375 + 180 μg/mL) against the pure drug combination, which is 9.26 ± 0.92 and 15.32 ± 1.08 IU/mL, respectively. The anti-inflammatory effects of liposomal formulations might be due to inhibition of T-cells by natural products because all drugs present in the formulation contain a substantial quantity of plant ITC and flavonoids, which were reported to produce anti-inflammatory action.

CRP values in case of NAR + PEITC CLFs get reduced from 16.25 ± 1.18 to 1.94 ± 0.42 mg/L as against 2.48 ± 0.40 mg/L for combination of free drugs (Figure 7D). Similar results were also observed for the NAR + SFN liposome against their free drug combination counterpart, which shows a decline in CRP levels of 4.75 ± 0.52 and 5.82 ± 0.65 mg/L, respectively. This indicates the strong anti-inflammatory potential of ITC (PEITC and SFN) to restore the animals to a normal condition possibly because of the Nrf2 inducer mechanism. However, blank liposome treatment did not show any healing effect.

2.8.1. Effects on the Oxidative Stress Biomarker. The arthritic rats showed approximately a threefold decrease in blood glutathione (GSH) and superoxide dismutase (SOD) levels, coupled with four fold decreases in the serum catalase level, indicating severe stress. This oxidative stress is a pathogenic hallmark in RA (caused by ROS), secreted from blood-derived cells and activated macrophages and is responsible for joint destruction leading to deformity. ITC and flavonoids have high antioxidant property as described previously in various reports.[46] In this manner, a combination of NAR with SFN and PEITC has the ability to decrease oxidative stress. This also reflected in our study (Figure 7E). FCA-induced oxidative biomarkers are attenuated by treatment with CLFs of NAR + PEITC to a greater extent, which is higher than their free drug combinations alone. However, the blank liposome composed of phospholipids does not show any pharmacological effect.

2.8.2. Effects on Hematological Parameters. The FCA-treated arthritic rats showed abnormal results with rise in the WBC count along with reduced RBC count and hemoglobin (Hb) concentration (Table 7).

The measured parameters indicated development of an anemic condition (iron deficiency), which is a clinical manifestation noted in RA. Both implemented liposomal treatments improved the anemic condition as marked by reversing back the hematological parameters to a normal range compared to the FCA-treated group [normal range of RBC (7.27−9.65 million/μL), WBC (1.96−8.25 million/μL), and Hb (13.7−17.6 g/dl) in male rats].[47]

There was approximately a 2.2-fold, 3.6-fold, and 3.7-fold increase in serum levels of SGOT, SGPT, and ALP levels, respectively, in the FCA-treated group in comparison to the vehicle control group (Table 7). It is worth noting that a substantial decrease in serum levels of SGOT, SGPT, and ALP to about a normal range of (74−143 U/mL), (62−230 U/mL) and (18−45 U/mL), respectively, was observed following the administration of CLFs (for 3 weeks) as compared to the FCA group ($p < 0.05$).

2.8.3. Measurement of Serum Proinflammatory (TNF-α, IL-6, INF-γ) and Anti-inflammatory Cytokine (IL-10). ITCs are well known for their promising anti-inflammatory activities. After stress-related cellular stimulation, the proinflammatory cytokines and I_kB are phosphorylated, leading to degradation of kinases. The NF-κB dimer gets free, is translocated into the nucleus, and transcription of proinflammatory cytokines (TNF-α, IL-6, INF-γ) gets induced. One of the proposed

https://dx.doi.org/10.1021/acsomega.0c04300
ACS Omega 2020, 5, 28319−28332

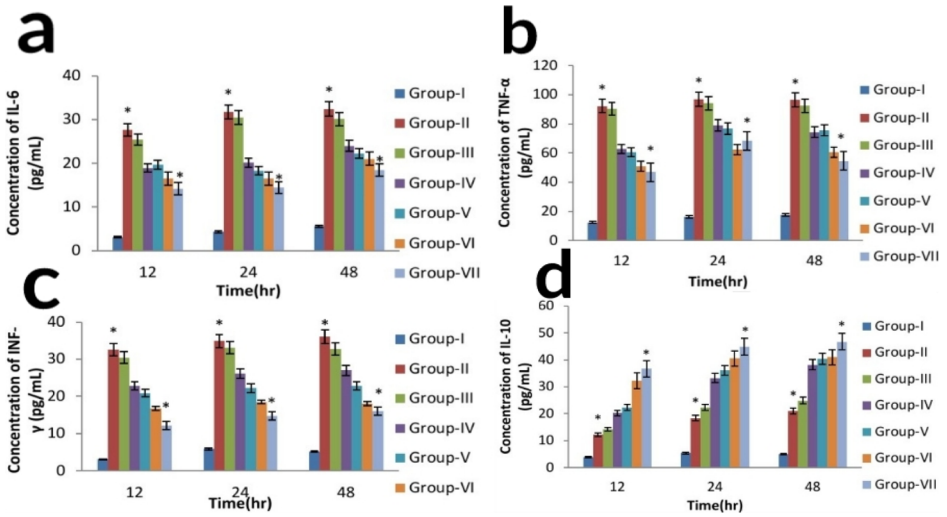

Figure 8. Effect of CLFs on proinflammatory cytokines (a) IL-6, (b) TNF-α, (c) INF-γ anti-inflammatory cytokines, (d) IL-10 on FCA-induced arthritic rats.

Table 8. Histological Scores of Rats

treatment	A (cell infiltration)	B (synovial hyperplasia)	C (pannus formation)	D (cartilage and bone erosion)
group I	0.15 ± 0.01	0.22 ± 0.02	0	0
group II	4.44 ± 0.12	3.92 ± 0.09	2.46 ± 0.04	1.77 ± 0.02
group III	4.62 ± 0.15	3.05 ± 0.12	2.82 ± 0.09	1.08 ± 0.04
group IV	2.64 ± 0.12	1.92 ± 0.04	0.98 ± 0.04	0.92 ± 0.02
group V	0.98 ± 0.03	0.84 ± 0.08	0.46 ± 0.04	0.42 ± 0.02
group VI	1.08 ± 0.04	1.07 ± 0.12	0.93 ± 0.09	0.89 ± 0.05
group VII	0.64 ± 0.06	0.52 ± 0.05	0.28 ± 0.02	0.25 ± 0.02

mechanisms of SFN and PEITC in reducing inflammation is attributed to the factor that they inhibit the activation of I_kB or inhibit NF-κB binding to DNA, thereby reducing the inflammation (arthritic). Previous reports also suggested that SFN and PEITC (ITCs) can significantly reduce several inflammatory mediators, for example, TNF-α, IL-6, INF-γ, nitric oxide (NO), and prostaglandin E (PGE_2), by suppressing activation of the NF-κB signaling pathway.[48]

Figure 8 depicts the consequence of CLFs, blank liposome, and free drug combination on inflammatory cytokines. It was investigated in the FCA-induced rat model by using sandwich ELISA. A great number of proinflammatory cytokines were released from rat peripheral blood mononuclear cells (PBMCs) upon induction of FCA. However, treatment of arthritic rats with both the prepared CLFs (NAR + SFN and NAR + PEITC) significantly decreased the proinflammatory cytokines levels and augmented the anti-inflammatory cytokine levels ($p < 0.05$), but a better effect was shown by the 15:4:1 NAR + PEITC liposome as shown in Figure 8. Both the pro- and anti-inflammatory cytokines are important regulators of synovial inflammation. Rheumatic inflammation is considered to be a biphasic process. The acute phase (first 10-day period) is due to the presence of mediators such as serotonin, histamine, kinins, and prostaglandins. These mediators are liberated through leucocytes and migrate toward the affected areas/regions. The chronic phase (10−21 days) is the second phase, which contributes to different cellular inflammatory mediators, that is, cytokines (IL-1β, IL-6, and TNF-α, INF-γ), granulocyte-macrophage colony-stimulating factors, and prostaglandins, respectively. In our study, the liposomal formulation of both NAR + SFN (ratio 2:1) and NAR + PEITC (ratio 1:1) inhibits pro-inflammatory cytokine IL-6, TNF-α, and INF-γ with simultaneous augmentation in anti-inflammatory cytokine IL-10 as compared to their free drug combination and blank liposome. The high grade of synovitis was noted from the results of histological analysis of ankle joints in FCA-induced rats (Table 8). The synovial hyperplasia score is increased in the FCA-induced arthritic rat, which is attenuated by CLFs significantly in comparison to their free drug combination. The high scores of cell infiltration and pannus formation are vital indicators in rheumatic degeneration. Cartilage with bone erosion is mainly caused by synoviocytes because of production of a matrix degradation enzyme.[49] If not treated in the stipulated period, later on, whole joints became disabled. As our results from Table 8 depict, the scores of cartilage and bone erosion, pannus formation, and cell infiltration get inhibited and resemble the normal control rat score with treatment of CLFs of NAR + PEITC/NAR + SFN. However, no change was observed for the blank liposome.

2.8.4. Histological Analysis of Ankle Joints. Untreated rats showed synovial hyperplasia and massive chronic inflammatory cells, suggesting cell infiltration with a marked loss of cartilage and bone (Figure 9). Synovial tissue is considered as one of the prime targets for any inflammatory disease. Inflammation in the synovial tissue leads to pannus formation. Usually, pannus tissue originates from the synovial lining consisting of synovial fibroblasts, synovial macrophages, and the activated T and B lymphocytes (inflammatory infiltration cells).[50] Although the drug treatment regimen significantly inhibited the acute joint destruction with granulocyte inflammation, chronic infiltration was reduced prominently by the group treated with CLF only,

https://dx.doi.org/10.1021/acsomega.0c04300
ACS Omega 2020, 5, 28319−28332

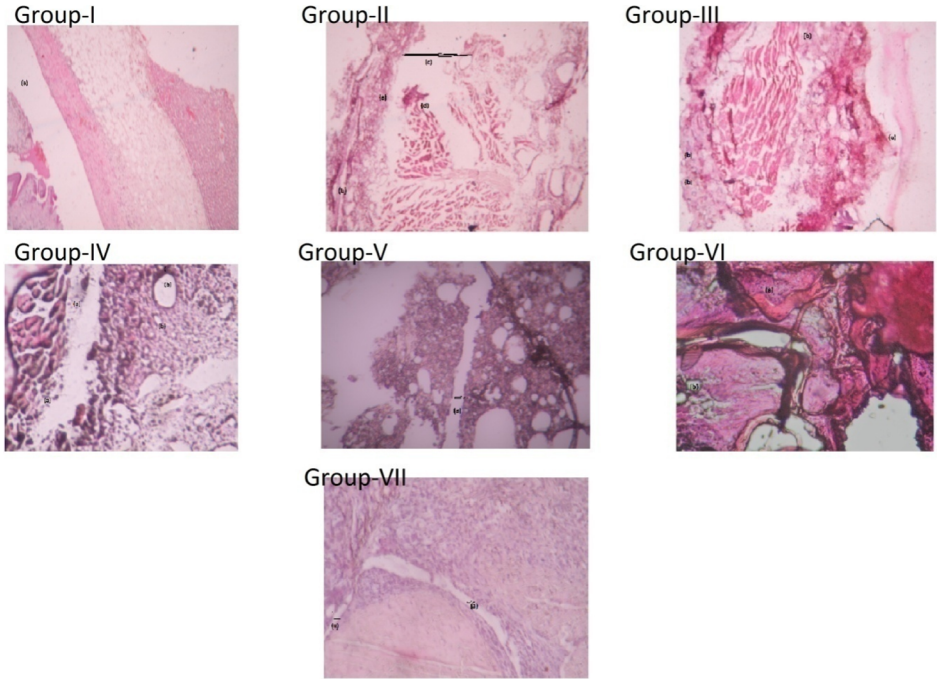

Figure 9. Histological analysis of an ankle joint stained with H and E stain. A Gr. I-healthy control rat shows normal articular surfaces with a smooth layer of cartilage (hyaline). A Gr. II-FCA-induced adjuvant arthritic rat showed (a) massive cell infiltration, (b) synovium, (c) joint cavity with a large joint space, (d) pannus formation, and (e) hyperanemia with dilated blood vessels. A Gr. III-FCA rat treated with the blank liposome showed (a) degradation of the articular surface and (b) infiltration of inflammatory cells. Gr. IV-in FCA rat treated with a combination of free drug NAR + SFN, (a) cellular infiltration is still present, which is composed of neutrophils representing acute inflammation and (b) vacuolar degeneration is also seen. Gr. V-in the synovial tissues treated with NAR + SFN CLF, fewer leukocytes were present and showed normal articular cartilage with (a) lesser joint space. Gr. VI-FCA rat treated with free drug combination of NAR + PEITC showed the presence of (a) cellular infiltration and (b) vacuolar degeneration. Gr. VII-adjuvant rat treated with NAR + PEITCCLF showing reduction of cell infiltration with (a) decrease in joint.

that is, NAR + PEITC and NAR + SFN, showing decrease in joint space. These effects were significantly stronger than those observed with free drug combinations.

3. CONCLUSIONS

Neither the blank liposome nor the combination of free drug (NAR + SFN)/(NAR + PEITC) could cause significant inhibition of proinflammatory markers and arthritic progression in FCA-induced rats. By contrast, the CLFs with both 15:4:1 NAR + SFN/NAR + PEITC could overcome acute and chronic inflammation. However, results were best seen with NAR + PEITC CLF. Notably, the composite liposome resulted in less joint tenderness with attenuation of bone erosion, thereby suggesting that the codelivery of flavonoid NAR with ITC (SFN/PEITC) generates a synergistic antiarthritic effect, irrespective of its multidrug resistance status. To our knowledge, this study is the first to apply this paradigm to evaluate drug combination therapy against RA.

4. MATERIALS AND METHODS

4.1. Materials. DPPC, cholesterol (chol), and DSPE-020CN (*N*-(carbonyl-methoxy polyethylene glycol 2000)-DSPE, sodium salt) were obtained as gift samples from Lipoid Company, Switzerland.

D,L-Sulforaphane (SFN) CAS no. 142825-10-3, purity >98%, PEITC CAS no. 2257-09-2, purity >98% and NAR (mol. wt 580.5 g/mol) CAS no. 10236-47-2 and FCA were procured from Sigma Aldrich Co. USA. Rat IL-6, IL-10, INF-γ, TNF-α, and ELISA kits were purchased from R&D Systems (Minneapolis, MN). All other chemicals used in the present study were of analytical grade.

4.2. Development of NAR + SFN and NAR + PEITC CLFs. CLFs of NAR + SFN and NAR + PEITC were prepared by a thin-film hydration method.[51] Different lipid ratios of DPPC/Chol/DSPE-020CN (15:0:1, 15:4:1, and 15:9:1) were used for studies. In brief, NAR mixed with the lipid mixture (in chloroform) was taken in glass test tubes. The organic solvent was evaporated under a stream of nitrogen gas and placed in a vacuum desiccator overnight to remove any residual organic solvent and resulting in a thin lipid film. The lipid films were then hydrated by adding water containing different concentrations of either PEITC or SFN and vortexed for 10 s. The rehydrated solution was then sonicated for 90 min to resuspend any precipitate and homogenize the sample. Finally, the sonicated sample is extruded using a polycarbonate membrane (pore size 100 nm) 21 times for size reduction. The prepared liposomes were dialyzed in precooled water (4 °C) at a 1:100 sample/sink ratio for 1 h using a 14,000 MWCO dialysis membrane to remove any free drug.

4.3. Physicochemical Characterization. *4.3.1. Determination of EE of SFN, NAR, and PEITC.* PEITC and SFN encapsulation is quantified using the cyclo-condensation reaction between ITC and BDT as per Zhang *et al.*[52] Potassium phosphate buffer of pH 8.5 containing 1% Triton X-100 is prepared to lyse the liposomes. The sample (100 μL), 500 μL of buffer, and 500 μL of 8 mM BDT are mixed and heated in a dry bath at 65 °C for 1 h. The solution is cooled to room temperature, centrifuged at 21,000*g* for 10 min, and the

https://dx.doi.org/10.1021/acsomega.0c04300
ACS Omega 2020, 5, 28319−28332

checked absorbance is measured at 365 nm. NAR quantification is done by mixing 100 μL of liposomal formulation with 450 μL each of methanol and water, respectively. This forms a 10× dilution of the sample to solubilize the lipid molecules and reduce the absorbance. Absorbance values are calculated at 283 nm and then multiplied by 10 to calculate the concentration of NAR in the sample.

EE is calculated by the following formula

$$\mathrm{EE} = \frac{\text{actual amount of drug encapsulated after dialysis}}{\text{total amount of drug added for encapsulation}} \times 100$$

4.3.2. Particle Size, Zeta Potential, and Polydispersity Index Analysis of NAR + SFN and NAR + PEITC CLFs. Dynamic light scattering was used to detect particle size, zeta potential, and polydispersity index at a room temperature of 25 °C using a Zetasizer Nano ZS (Malvern Instruments, Malvern, UK).

4.3.3. FT-IR Analysis. FT-IR spectra of free drugs NAR, SFN, and PEITC, blank liposome composed of phospholipids DPPC/Chol/DSPE-020CN in a 15:0:1/15:4:1/15:9:1 M ratio, and coloaded liposome of a 15:4:1 M ratio (NAR + SFN) and (NAR + PEITC) were analyzed using an FT-IR spectrophotometer (Thermo Fisher Scientific) in which the disk of each sample was individually scanned over a wavelength of 500−4000/cm.

4.3.4. DSC Analysis. DSC (Pyris Diamond DSC, PerkinElmer) was used to record the thermal behavior of blank liposomes, a free drug combination (NAR + SFN/NAR + PEITC), and co-loaded (15:4:1 NAR + SFN/NAR + PEITC) liposomes. The samples were loaded on the aluminum pans and scanned in a range from 0 to 250 °C with a scan rate of 10 °C/min.

4.3.5. XRD analysis. XRD analysis was carried out using an X-ray diffractometer; Diano, Woburn, USA, at 45 kV, 9 mA at an angle of 2θ for blank liposomes, free drug combination, and coloaded liposomes.

4.3.6. In Vitro Release Studies. A dialysis method was adopted to study the release kinetics of the prepared formulations.[53] The prepared liposomal samples (1 mL) were taken in 10 mL of phosphate-buffered saline (PBS) at pH 7.4 and stirred at 300 rpm at room temperature. An aliquot of 60 μL was taken at a predetermined time interval and replaced with the same volume of PBS. The samples are taken every half hour for the first 6 h and then taken every hour for the next 6, 24, and 48 h respectively and an equal volume of dissolution medium was added to the bottle. The detection was carried out as follows.

4.3.6.1. NAR Detection. A NAR standard curve is prepared from 1 to 10 μg/mL at 283 nm. In the 30 μL sample, 30 μL of water and 30 μL of methanol are added to make the volume 90 μL. The sample is then centrifuged at 21,000*g* for 10 min. The sample absorbance is checked using the standard curve and multiplied by 3 to compensate for the dilution.

4.3.6.2. ITC (PEITC and SFN) Detection. ITC release is measured by mixing 30 μL of the sample, 30 μL of BDT (8 mM) dissolved in methanol, and 30 μL of potassium phosphate buffer at pH 8.5. The sample is heated at 65 °C for 1 h and then centrifuged at 21,000*g* for 10 min. The absorbance of the supernatant is taken at 365 nm. The release data were fitted to the different drug-release kinetic models, that is, zero-order, first-order, Higuchi, Hixon−Crowell, and Korsmeyer Peppas models. The corresponding linear regression coefficients (R^2) were determined in order to know the release mechanism.[54]

4.4. *In Vivo* Studies. *4.4.1. Animal Procurement and Maintenance.* Healthy, adult male Wistar rats (150−200g) were used for the research, which were obtained from the animal house of Siksha "O" Anusandhan (deemed to be university) Bhubaneswar, Odisha. The animals were kept under appropriate conditions and are maintained in a natural habitat, fed with palate diet, and provided potable water as mentioned in the CPCSEA guidelines.

4.4.1.1. Experimental Design. Two models of inflammation were used to study the *in vivo* performance of the prepared CLFs and the study was approved by the Animal Ethical Committee of the School of Pharmaceutical Sciences, SOA (deemed to be university), Bhubaneswar. Odisha (IAEC/SPS/SOA/15/2018).

(a) Assessment of anti-inflammatory activity was done using acute models of inflammation (carrageenan-induced rat paw edema model/histamine-induced rat paw edema model/egg albumin-induced rat paw edema model) (one day treatment 0−6 h).

(b) Assessment of antiarthritic activity was done using a chronic model of inflammation (FCA-induced arthritic rat model) (21-day treatment).

The animal models were distributed equally into seven groups. Each group received intraperitoneal (IP) injection as follows: group I contains normal rats; group II is the toxic control-carrageenan/histamine/egg albumin/FCA-induced rats; group III rats receive blank liposome (without a drug) + toxic control; group IV rats were treated with a combination of free drug NAR + SFN (375 +180 μg/mL) in a ratio of 2:1 + toxic control; group V rats receive coloaded liposome in a 15:4:1 M ratio NAR + SFN (375 + 180 μg/mL) ratio 2:1 + toxic control; group VI rats treated with a free drug combination of NAR + PEITC (375 + 375 μg/mL) in a ratio of 1:1 + toxic control; and group VII rats were treated with a coloaded liposome in a 15:4:1 M ratio of NAR + PEITC (375 + 375 μg/mL) ratio 1:1 + toxic control (n = 6 in each group).

4.4.1.2. Acute Inflammatory Model. Carrageenan/histamine/egg albumin-induced rat paw edema model: carrageenan/histamine/egg albumin (0.1 mL of 1%) was injected into the subplantar tissue of the right hind paw of each rat. The volume of the carrageenan/histamine/egg albumin injected into the foot was measured at the 0, first, third, and sixth hour using a plethysmometer (Bio Devices, New Delhi).[55]

Chronic inflammatory model: On the first day, excluding group I, all the other groups of rats were given a single dose of 0.1 mL of FCA intradermally into the right hind paw and arthritis was induced in the animals. After this day, blank liposome, a combination of free drugs and CLFs were administered to the rats *via* the IP route for up to 21 days. Arthritis progression was monitored every day and special care was taken to ensure that the rats had adequate access to food and water during disease progression.

Measurement of arthritic score and paw volume: The severity of RA was evaluated from the paw of animals and was graded from zero to four. Structural characteristic of the arthritis (*i.e.*, redness, inflammation, erythema) were observed by visual inspection. These were graded as normal paw = grade 0, digits with mild swelling and erythema = grade 1, digits with

https://dx.doi.org/10.1021/acsomega.0c04300
ACS Omega 2020, 5, 28319−28332

swelling and redness = grade 2, severe swelling and redness = grade 3, inability to use the limb with gross deformity = grade 4 on respective days. It was observed that the maximum possible score for both hind paws was 8. All animals' right hind paw volume was observed at various time intervals, that is, just before administration of FCA (on day 0) and thereafter at different time intervals till day 21 using a plethysmometer.[56] Based on the final and initial paw volumes, the distinction was observed at an interval of every 7 days.

Measurement of biochemical and hematology parameters: At the end of the experimental period (*i.e.*, on 22nd day), the animals were sacrificed; blood was withdrawn by piercing the cardiac and kept in two different tubes, one containing EDTA (anticoagulant) and another tube without anticoagulant. Serum was separated and used for estimation of liver marker enzymes (SGPT, SGOT, ALP) using standard laboratory procedures. Observations of CRP and RF levels were obtained. The hematological parameters such as WBC, RBC, and Hb were also measured.[57]

Estimation of levels of antioxidant: GSH levels were evaluated to estimate the endogenous defence against oxidative stress. The method was based on Ellman's reagent (DTNB) reaction with the free thiol group. EDTA (0.02 M) and 50% trichloro acetic acid solution were added to the serum sample. After centrifugation (3000 rpm/15 min), the supernatant was collected and production levels of GSH were evaluated as described by Sedlack and Lidsay. To the samples were added 0.4 Tri-HCl buffer, pH 8.0, and 0.01 M DTNB. GSH levels were determined at 412 nm and reported (Ellman *et al.* 1976).[58]

Catalase activity was determined by the method that employs hydrogen peroxide (H_2O_2) to generate H_2O and O_2. The standard assay substrate mixture contained 0.30 mL of H_2O_2 in 50 mL of 0.05 M phosphate buffer, pH 7.0. To 980 μL of the substrate mixture, 20 μL of the sample was added, absorbance was recorded at 240 nm, and results were expressed (Chance *et al.* 1955).[59]

SOD enzyme activity was calculated in plasma according to the method of Misra and Fridovich (1972) with slight modifications. SOD levels were determined at 460 nm and results expressed as U/mg protein.[60]

Measurement of inflammatory cytokines (TNF-α, IL-6, INF-γ, IL-10): Blood was withdrawn from experimental rats. The serum was revived and chilled at −20 °C until evaluation. The protein concentrations of serum proinflammatory cytokines such as TNF-α, IL-6, INF-γ, and anti-inflammatory cytokine (IL-10) were calibrated by ELISA based on the protocols of the manufacturer.

Briefly, rat peripheral blood was obtained from both adjuvant-treated and untreated (normal control) rats. It was kept in sterile sodium heparin tubes and mixed with PBS (pH-7.4) and Ficoll-Paque PLUS (GE Healthcare) in order to obtain PBMCs. The heparinized blood was centrifuged at 2000 rpm for 20 min at 15 °C to obtain a PBMC ring. Thereafter, the obtained PBMC (in ring form) was centrifuged by mixing it with PBS and fetal bovine serum (FBS) (1000 rpm, 20 min, 15 °C) to obtain a leukocyte cloud. From the inter phase, cells of PBMC were extracted and washed three times with PBS for 10 min (1000 rpm, 15 °C) and were allowed to be cultured in Roswell Park Memorial Institute (RPMI) 1640 medium with 20 mm Hepes supplemented with 10% FBS, Hi Media after the last wash. The number of PBMCs were counted using a hemocytometer.

Cell proliferation assays: Cell proliferation assays were performed using an MTT assay kit (eBioscience) as per the instructions of the manufacturer. Cultured PBMCs were resuspended (5×10^6 cells/mL) in RPMI 1640 medium in the presence of lipopolysaccharide. Then, 100 μL of different concentrations of both treated and untreated samples were added in RPMI-1640. Incubation of the cultured plates was carried out for 48 h in a CO_2 incubator (5% CO_2 and 37 °C temperature). To each well, around 10 μL of MTT (3[4,5-dimethylthiazol-2-yl]-2,5-diphenyltetrazolium bromide (2.5 mg/mL) solution was added, and the plates were wrapped to avoid exposure to light. Incubation is allowed for 4 h where 100 μL of the solubilizing reagent was added in each well. Finally, absorbance was recorded at 570 nm using a Mind ray MR-96A microplate absorbance reader.[61]

Histological analysis: All joints cleansed with saline were fixed with 10% formalin solution and sections of proximal ankle joints were stained with hematoxylin and eosin for a general histological evaluation to view any cartilage damage. Finally, they were viewed in 40× magnification.[62]

Histological scores from 0 to 5 were given for each joint with respect to cell infiltration, synovial hyperplasia, pannus formation, and cartilage erosion, respectively.

Statistical analysis: All outcomes were expressed as mean ± SEM (n = 6). The significance of distinction between the treated groups was determined using Dunnet's t-test. In ANOVA, a p value < 0.05 was considered as significant..

AUTHOR INFORMATION

Corresponding Authors

Sangeeta Mohanty − *School of Pharmaceutical Sciences, Siksha O Anusandhan Deemed to Be University, Bhubaneswar 751030, India;* orcid.org/0000-0002-4539-0570; Email: sangeetamohanty12@gmail.com

V. Badireenath Konkimalla − *School of Biological Sciences, National Institute of Science Education and Research, HBNI, Jatni, Odisha 752050, India*; Email: badireenath@niser.ac.in

Authors

Ashish Kumar Sahoo − *School of Biological Sciences, National Institute of Science Education and Research, HBNI, Jatni, Odisha 752050, India*

Abhisek Pal − *Gitam School of Pharmacy, Gitam Deemed to Be University, Hyderabad 502329, India*

Sudam Chandra Si − *School of Pharmaceutical Sciences, Siksha O Anusandhan Deemed to Be University, Bhubaneswar 751030, India*

Complete contact information is available at: https://pubs.acs.org/10.1021/acsomega.0c04300

Author Contributions

S.M. and A.K.S. contributed equally to this work. Design of work was done by V.B.K. and S.M. Formulation studies were conducted by V.B.K. and A.K.S. Characterization and pharmacological studies were performed by S.M. Histology and pharmacology data analysis was performed by A.P. Reagents were contributed by S.C.S. The paper was written by S.M.

Notes

The authors declare no competing financial interest.

https://dx.doi.org/10.1021/acsomega.0c04300
ACS Omega 2020, 5, 28319−28332

■ ACKNOWLEDGMENTS

This work was supported by the National Institute of Science Education and Research (NISER) and School of Pharmaceutical Sciences, SOA Deemed to be University, Bhubaneswar, Odisha.

■ REFERENCES

(1) Firestein, G. S. Evolving concepts of rheumatoid arthritis. *Nature* **2003**, *423*, 356−361.
(2) Smolen, J. S.; Steiner, G. Therapeutic strategies for rheumatoid arthritis. *Nat. Rev. Drug Discovery* **2003**, *2*, 473−488.
(3) Hu, C.-M.; Zhang, L. Therapeutic nanoparticles to combat cancer drug resistance. *Curr. Drug Metab.* **2009**, *10*, 836−841.
(4) Liang, X. J.; Chen, C. Y.; Zhao, Y. L.; Wang, P. C. Circumventing Tumor Resistance to Chemotherapy by Nanotechnology. *Multi-Drug Resistance in Cancer*; Zhou, J., Ed.; Methods in Molecular Biology; Humana Press, 2010; Vol. *596*; pp 467−488.
(5) Bharti, S.; Rani, N.; Krishnamurthy, B.; Arya, D. Preclinical evidence for the pharmacological actions of naringin: a review. *Planta Med.* **2014**, *80*, 437−451.
(6) Benavente-García, O.; Castillo, J. Update on uses and properties of citrus flavonoids: new findings in anticancer, cardiovascular, and anti-inflammatory activity. *J. Agric. Food Chem.* **2008**, *56*, 6185−6205.
(7) Chanet, A.; Milenkovic, D.; Manach, C.; Mazur, A.; Morand, C. Citrus flavanones: what is their role in cardiovascular protection? *J. Agric. Food Chem.* **2012**, *60*, 8809−8822.
(8) Ahmad, S. F.; Zoheir, K. M. A.; Abdel-Hamied, H. E.; Ashour, A. E.; Bakheet, S. A.; Attia, S. M.; Abd-Allah, A. R. A.; et al. Amelioration of autoimmune arthritis by naringin through modulation of Tregulatory cells and Th 1/Th2 cytokines. *Cell. Immunol.* **2014**, *287*, 112−120.
(9) Aras, U.; Gandhi, Y. A.; Masso-Welch, P. A.; Morris, M. E. Chemopreventive and anti-angiogenic effects of dietary phenethyl isothiocyanate in an N-methyl nitrosourea-induced breast cancer animal model. *Biopharm. Drug Dispos.* **2013**, *34*, 98−106.
(10) Yadav, M.; Sehrawat, N.; Singh, M.; Upadhyay, S.; Diwakar, A.; Sharma, A. Cardioprotective and Hepatoprotective Potential of Citrus Flavonoid Naringin: Current Status and Future Perspectives for Health Benefits. *Asian J. Biol. Life Sci.* **2020**, *9*, 1−5.
(11) Aras, U.; Gandhi, Y. A.; Masso-Welch, P. A.; Morris, M. E. Chemopreventive and anti-angiogenic effects of dietary phenethyl isothiocyanate in an N-methyl nitrosourea-induced breast cancer animal model. *Biopharm. Drug Dispos.* **2013**, *34*, 98−106.
(12) Chung, F. L.; Morse, M. A.; Eklind, K. I.; Lewis, J. Quantitation of human uptake of the anticarcinogen phenethyl isothiocyanate after a watercress meal. *Cancer Epidemiol. Biomark. Prev.* **1992**, *1*, 383−388.
(13) Choudhary, N.; Gupta, R.; Bhatt, L. K. Anti-rheumatic activity of Phenethyl isothiocyanate via inhibition of histone deacetylase-1. *Chem.-Biol. Interact.* **2020**, *324*, 109095.
(14) Srivastava, R. K.; Tang, S. N.; Zhu, W.; Meeker, D.; Shankar, S. Sulforaphane synergizes with quercetin to inhibit self-renewal capacity of pancreatic cancer stem cells. *Front. Biosci.* **2011**, *3*, 515−528.
(15) Silva Rodrigues, J. F.; e Silva, C. S.; França Muniz, T.; de Aquino, A.; Neuza, S.; Nina, L.; Fialho Sousa, N. C.; Nascimento Silva, L. N.; Souza, B. G.; Penha, T. A.; Abreu-Silva, A. L.; Sá, J. C.; Soares Fernandes, E.; Grisotto, M. A. Sulforaphane Modulates Joint Inflammation in a Murine Model of Complete Freund's Adjuvant-Induced Mono. *Molecules* **2018**, *23*, 988.
(16) De Figueiredo, S.; Binda, N.; Nogueira-Machado, J.; Vieira-Filho, S.; Caligiorne, R. The antioxidant properties of organosulfur compounds (sulforaphane). *Recent Pat. Endocr. Metab. Immune Drug Discov.* **2015**, *9*, 24−39.
(17) Fragoulis, A.; Laufs, J.; Müller, S.; Soppa, U.; Siegl, S.; Reiss, L.; Tohidnezhad, M.; Rosen, C.; Tenbrock, K.; Varoga, D.; Lippross, S.; Pufe, T.; Wruck, C. Sulforaphane has opposing effects on TNF-alpha stimulated and unstimulated synoviocytes. *Arthritis Res. Ther.* **2012**, *14*, R220.
(18) Petri, S.; Körner, S.; Kiaei, M. Nrf2/ARE Signaling Pathway: Key Mediator in Oxidative Stress and Potential Therapeutic Target in ALS. *Neurol. Res. Int.* **2012**, *2012*, 878030.
(19) Chia-Fa, L.; Tsung-Hung, C.; Cheng-Hsun, C.; Shue-Dong, C.; Tzu-Ching, C.; Chiang-Ting, C. Sulforaphane improves voiding function via the preserving mitochondrial function in diabetic rats. *J. Formos. Med. Assoc.* **2020**, *119*, 1422−1430.
(20) Kaboli, P. J.; Khoshkbejarid, M. A.; Mohammadie, M.; Abirif, A.; Mokhtarianc, R.; Vazifemandg, R.; Amanollahic, S.; Sani, S. Y.; Li, M.; Zhaoa, Y.; Wu, X.; Shena, J.; Cho, C. H.; Xiao, Z.; et al. Targets and mechanisms of sulforaphane derivatives obtained from cruciferous plants with special focus on breast cancer − contradictory effects and future perspectives. *Biomed. Pharmacother.* **2020**, *121*, 109635.
(21) Houghton, C. A. Sulforaphane: "Its coming of Age" as a clinically relevant nutraceutical in the prevention and treatment of chronic disease. *Oxid. Med. Cell. Longevity* **2019**, *2019*, 2716870.
(22) Hu, R.; Hebbar, V.; Kim, B.-R.; Chen, C.; Winnik, B.; Buckley, B.; Soteropoulos, P.; Tolias, P.; Hart, R. P.; Kong, A.-N. T. In vivo pharmacokinetics and regulation of gene expression profiles by isothiocyanate sulforaphane in the rat. *J. Pharmacol. Exp. Therapeut.* **2004**, *310*, 263−271.
(23) Mohanty, S.; Pal, A.; Konkimalla, V. B.; Chandra Si, S. Anti-inflammatory and anti-granuloma activity of sulforaphane, a naturally occurring isothiocyanate from broccoli (brassica-oleracea). *Asian. J. Pharm. Clin. Res.* **2018**, *11*, 411−416.
(24) Mohanty, S.; Pal, A.; Sharma, T.; Singh, S.; Konkimalla, V. B.; Si, S. C. Anti-arthritic effect of Sulforaphane (SFN) in FCA-induced arthritic rats by suppressing pro-inflammatory cytokines and tissue regeneration. *Int. J. Curr. Pharmaceut. Res.* **2020**, *12*, 394−399.
(25) Bangham, A. D.; Horne, R. W. Negative staining of phospholipids and their structural modification by surface-active agents as observed in the electron microscope. *J. Mol. Biol.* **1964**, *8*, 660.
(26) Harrington, K. J.; Rowlinson-Busza, G.; Syrigos, K. N.; Vile, R. G.; Uster, P. S.; Peters, A. M.; Stewart, J. S. Pegylated liposome-encapsulated doxorubicin and cisplatin enhance the effect of radiotherapy in a tumor xenograft model. *Clin. Cancer Res.* **2000**, *6*, 4939−4949.
(27) Hu, C.-M.; Zhang, L.; et al. Therapeutic nanoparticles to combat cancer drug resistance. *Curr. Drug Metab.* **2009**, *10*, 836−841.
(28) Ren, H.; He, Y.; Liang, J.; Cheng, Z.; Zhang, M.; Zhu, Y.; Hong, C.; Qin, J.; Xu, X.; Wang, J. Role of Liposome Size, Surface Charge, and PEGylation on Rheumatoid Arthritis Targeting Therapy. *ACS Appl. Mater. Interfaces* **2019**, *11*, 20304−20315.
(29) Kolate, A.; Baradia, D.; Patil, S.; Vhora, I.; Kore, G.; Misra, A. PEG - a versatile conjugating ligand for drugs and drug delivery systems. *J. Controlled Release* **2014**, *192*, 67−81.
(30) Koning, G. A.; Schiffelers, R. M.; Wauben, M. H. M.; Kok, R. J.; Mastrobattista, E.; Molema, G.; et al. Targeting of angiogenic endothelial cells at sites of inflammation by dexamethasone phosphate-containing RGD peptide liposomes inhibits experimental arthritis. *Arthritis Rheum.* **2006**, *54*, 1198−1208.
(31) Cordenonsi, L. M.; Sponchiado, R. M.; Campanharo, S. C.; Garcia, C. V.; Raffin, R. P.; Schapoval, E. E. S. Study of flavonoids present in Pomelo (Citrus máxima) by DSC, UV-VIS, IR,^{1}H and^{13}C NMR and MS. *Drug Anal. Res.* **2017**, *1*, 31−37.
(32) Lieber, E.; Rao, C. N. R.; et al. The infrared spectra of organic thiocyanates and isothiocyanates. *Spectrochim. Acta* **1959**, *13*, 296−299.
(33) Gupta, U.; Vivek, K.; Kumar, V.; Khajuria, Y.; et al. Spectroscopic Studies of Cholesterol: Fourier Transform Infra-Red and Vibrational Frequency Analysis. *Mater. Focus* **2014**, *3*, 211−217.
(34) Yuan, H.-N.; Yao, S. J.; Shen, L. Q.; Mao, J. W. Preparation and Characterization of Inclusion Complexes of β - Cyclodextrin -BITC and β-Cyclodextrin −PEITC. *Ind. Eng. Chem. Res.* **2009**, *48*, 5070.
(35) Seddon, J. M.; Cevc, G.; Marsh, D.; et al. Calorimetric studies of the gel-fluid (L.beta.-L.alpha.) and lamellar-inverted hexagonal

https://dx.doi.org/10.1021/acsomega.0c04300
ACS Omega 2020, 5, 28319−28332

(L.alpha.-HII) phase transitions in dialkyl- and diacylphosphatidylethanolamines. *Biochemistry* **1983**, *22*, 1280−1289.
(36) Mabrey, S.; Mateo, P. L.; Sturtevant, J. M. High-sensitivity scanning calorimetric study of mixtures of cholesterol with dimyristoyl and dipalmitoylphosphatidylcholines. *Biochemistry* **1978**, *17*, 2464−2468.
(37) Cordenonsi, L. M.; Sponchiado, R. M.; Campanharo, S. C.; et al. Study of flavonoids present in Pomelo (Citrus máxima) by DSC, UV-VIS, IR, ^{1}H AND ^{13}C NMR AND MS. *Drug Anal. Res.* **2017**, *1*, 31−37.
(38) Malathy, S.; Iyer, P. R.; et al. Naringin Loaded Chitosan Nanoparticle for Bone Regeneration: A Preliminary in vitro study. *J. Nanomed. Nanotechnol.* **2018**, *9*, 4.
(39) Mohamed, E.; Abu Hashim, I.; Yusif, R.; Shaaban, A.; El-Sheakh, A.; Hamed, M.; Badria, F. Polymeric micelles for potentiated antiulcer and anticancer activities of naringin. *Int. J. Nanomed.* **2018**, *13*, 1009−1027.
(40) Yuan, H.-N.; Yao, S.-J.; Shen, L.-Q.; et al. Preparation and Characterization of Inclusion Complexes of Cyclodextrin-BITC and Cyclodextrin-PEITC. *Ind. Eng. Chem. Res.* **2009**, *48*, 5070−5078.
(41) Payan, D. G.; Shearn, M.; et al. A non steroidal anti-inflammatory drugs: Non opioid analgesics: Drugs used in gout. *Basic and Clinical Pharmacology*; Katzung, B. G., Eds.; Appleton and Lange: USA, 1989; pp 431−450.
(42) Linardi, A.; Costa, S. K. P.; da Silva, G. R.; Antunes, E. Involvement of kinins, mast cells and sensory neurons in the plasma exudation and paw oedema induced by staphylococcal enterotoxin B in the mouse. *Eur. J. Pharmacol.* **2000**, *399*, 235−242.
(43) Yankanchi, S. R.; Koli, S. A.; et al. Anti-inflammatory and analgesic activity of mature leaves of methanol extract of Clerodendruminerme L. (Gaertn). *J. Pharm. Sci. Res.* **2010**, *11*, 782−785.
(44) Scott, D. L.; Wolfe, F.; Huizinga, T. W. Rheumatoid arthritis. *Lancet* **2010**, *376*, 1094.
(45) Guha, P.; Subhashis, P.; Das, A.; Halder, B.; Bhattacharjee, S.; Chaudhury, T. Analyses of Human and Rat Clinical Parameters in Rheumatoid Arthritis Raise the Possibility of Use of Crude Aloe vera Gel in Disease Amelioration. *Immunome Res.* **2014**, *10*, 081.
(46) Kolm, R. H.; Danielson, U. H.; Zhang, Y.; Talalay, P.; Mannervik, B. Isothiocyanates as substrates for human glutathione transferases. *Biochem. J.* **1995**, *311*, 453−459.
(47) Shehani, L.; Delwatta, M. G.; Vera, B.; et al. Reference values for selected hematological, biochemical and physiological parameters of Sprague-Dawley rats at the Animal House, Faculty of Medicine, University of Colombo, Sri Lanka. *Anim. Model Exp. Med.* **2018**, *1*, 250−254.
(48) Ruhee, R. T.; Suzuki, K.; et al. The Integrative Role of Sulforaphane in Preventing Inflammation, Oxidative Stress and Fatigue: A Review of a Potential Protective Phytochemical. *Antioxidants* **2020**, *9*, 521.
(49) Fragoulis, A.; Laufs, J.; Müller, S.; Soppa, U.; Siegl, S.; Reiss, L.; Tohidnezhad, M.; Rosen, C.; Tenbrock, K.; Varoga, D.; Lippross, S.; Pufe Wruck, C. J.; et al. Sulforaphane has opposing effects on TNF-alpha stimulated and unstimulated synoviocytes. *Arthritis Res. Ther.* **2012**, *14*, R220.
(50) Kolm, R. H.; Danielson, U. H.; Talalay, P.; Mannervik, B.; Mannervik, B. Isothiocyanates as substrates for human glutathione transferases. *Biochem. J.* **1995**, *311*, 453−459.
(51) Zhang, H.; et al. Thin-Film Hydration Followed by Extrusion Method for Liposome Preparation. *Methods Mol. Biol.* **2017**, *1522*, 17−22.
(52) Zhang, Y.; et al. The 1,2-Benzenedithiole-Based Cyclocondensation Assay, a valuable tool for measurement of chemopreventive isothiocyanates. *Crit. Rev. Food Sci. Nutr.* **2012**, *52*, 525−532.
(53) Wang, Q.; Jiang, J.; Chen, W.; Jiang, H.; Zhang, Z.; Sun, X.; et al. Targeted delivery of low-dose dexamethasone using PCL-PEG micelles for effective treatment of rheumatoid arthritis. *J. Controlled Release* **2016**, *230*, 64−72.
(54) Narayanan, S.; Pavithran, M.; Viswanath, A.; Narayanan, D.; Mohan, C. C.; Manzoor, K.; Menon, D. Sequentially releasing dual-drug-loaded PLGA-casein core/shell nanomedicine: design, synthesis, biocompatibility and pharmacokinetics. *Acta Biomater.* **2014**, *10*, 2112−2124.
(55) Winter, C. A.; Risley, E. A.; Nuss, G. W.; et al. Carrageenin-induced edema in the hind paw of rat as an assay for anti-inflammatory drugs. *Proc. Soc. Exp. Biol. Med.* **1962**, *111*, 544−547.
(56) Fereidoni, M.; Ahmadiani, A.; Semnanian, S.; Javan, M. An accurate and simple method for measurement of paw edema. *J. Pharmacol. Toxicol. Methods* **2000**, *43*, 11−14.
(57) Mehta, A.; Sethiya, N. K.; Mehta, C.; Shah, G. Anti-arthritis activity of roots of Hemidesmus indicus R.Br. (Anantmul) in rats. *Asian Pac. J. Trop. Med.* **2012**, *5*, 130−135.
(58) Sinha, A. K.; et al. Colorimetric assay of catalase. *Anal. Biochem.* **1972**, *47*, 389−394.
(59) Datta, P.; Amrita, S.; Ajoy, K. B.; Antony, G.; et al. Anti arthritic activity of aqueous extract of Indian black tea in experimental and clinical study. *Orient. Pharm. Exp. Med.* **2012**, *12*, 265−271.
(60) Sternberg, M.; Peyroux, J.; Grochulski, A.; Engler, R.; Feret, J.; et al. Biochemical criteria for the evaluation of drug efficiency on adjuvant arthritis and nephrotoxic serum nephritis in the rat: studies with phenyl butazone, L-Asparaginase, colchicine, lysine acetylsalicylate, and pyridinol carbamate. *Can. J. Physiol. Pharmacol.* **1975**, *53*, 368−374.
(61) Singh, U.; Tabibian, J.; Venugopal, S. K.; Devaraj, S.; Jialal, I.; et al. Development of an in vitro screening assay to test the anti-inflammatory properties of dietary supplements and pharmacologic agents. *Clin. Chem.* **2005**, *51*, 2252−2256.
(62) Banji, D.; Banji, O. J. F.; Saidulu, A.; Hayath, M. S.; et al. Synergistic activity of curcumin with methotrexate in ameliorating Freund's Complete Adjuvant induced arthritis with reduced hepatotoxicity in experimental animals. *Eur. J. Pharmacol.* **2011**, *668*, 293−298.

https://dx.doi.org/10.1021/acsomega.0c04300
ACS Omega 2020, 5, 28319−28332